Journal of Magnetic Resonance 210 (2011) 107–112

Contents lists available at ScienceDirect

Journal of Magnetic Resonance

journal homepage: www.elsevier.com/locate/jmr

Creation and evolution of net proton hyperpolarization arising from para-hydrogenation

Francesca Reineri [a], Sabine Bouguet-Bonnet [b], Daniel Canet [b,*]

[a] Dipartimento di Chimica I.F.M. and Center for Molecular Imaging, Università Degli Studi di Torino, Via P. Giuria 7, 10125 Torino, Italy
[b] Méthodologie RMN (CRM2, UMR 7036 CNRS-UHP), Université Henri Poincaré, BP 239, 54506 Vandoeuvre-lés-Nancy Cedex, France

ARTICLE INFO

Article history:
Received 18 January 2011
Revised 16 February 2011
Available online 23 February 2011

Keywords:
PHIP
Hyperpolarization
paraHydrogen
Spin relaxation

ABSTRACT

When a hydrogenation reaction is carried out with gaseous hydrogen enriched in its para- isomer in the earth magnetic field (prior to adiabatic insertion of the sample in the NMR magnet), enhanced proton longitudinal order (represented by $2I_z^AI_z^B$) is created but also difference of enhanced polarizations ($I_z^A - I_z^B$). In a first part, it is shown theoretically and experimentally that the longitudinal relaxation time of this polarization difference is roughly twice the ones of individual polarizations. The second part is devoted to a pulse sequence designed for transforming this difference into net hyperpolarization. The evolution of this global hyperpolarization is studied experimentally in a third part and it is observed that a fraction of hyperpolarization possesses an effective longitudinal relaxation time similar to the one of the initial polarization difference. Those experimental results are interpreted by numerical calculations based on Solomon-type equations including the longitudinal order and possibly dipolar-csa cross correlation rates.

1. Introduction

Biomedical applications (especially MRI) of ParaHydrogen (pH_2) Induced Polarization (PHIP) [1] make generally use of ^{13}C hyperpolarization. This hyperpolarization originates from the protons of an appropriate molecule which has been subjected to a hydrogenation reaction by gaseous hydrogen enriched in its para isomer. The main reason is that ^{13}C nuclei have generally relaxation times longer than those of protons, thus enabling more time for imaging experiments [2] (which, in addition, will not be perturbed by the strong water proton signal). Moreover protons can be in a complicated spin state, involving at least longitudinal spin orders (see below). Indeed, the problem is to transform the proton spin state into ^{13}C hyperpolarization. A first approach is an INEPT-like pulse sequence [3–6]. Field cycling procedures [2,7] or special pulse sequences [8,9] constitute other ways of achieving ^{13}C hyperpolarization by transfer from enhanced proton spin states. These special pulse sequences have been systematically used in very recent works devoted to biomedical applications of NMR and MRI [10–12]. However, even if the totality of hyperpolarization is transferred, ^{13}C imaging, with respect to ^1H imaging, entails a sensitivity loss by a factor of 16 (the square of the gyromagnetic constants ratio). This is a strong incitement for employing directly proton hyperpolarization, provided that the spin states can be really transformed into net hyperpolarization. It is the very problem we address in this work. Indeed, for a two spin ½ system, in addition to the longitudinal spin order (represented by the operator product $2I_z^AI_z^B$, where *A* and *B* are two spins originating from pH_2), one may observe a polarization difference (represented by $I_z^A - I_z^B$). As a matter of fact, PASADENA [13] experiments (hydrogenation reaction inside the NMR magnet) yield only longitudinal order while ALTADENA [14] experiments can produce both longitudinal order and polarization difference, [1,14–16]. Longitudinal spin order can be transformed into an observable signal by a radio-frequency (rf) pulse of flip angle smaller than 90° (maximum obtained with a 45° flip angle). The observable signal is however an anti-phase doublet which implies the existence of a J coupling between *A* and *B*. This anti-phase doublet is evidently not suitable for most applications since it may not be resolved due to a low value of the J coupling and/or to the static field inhomogeneity. Moreover, it is *not* a polarization. We have therefore to rely on the polarization difference ($I_z^A - I_z^B$). Again it is *neither* a net polarization since *A* and *B* may have opposite effects (in imaging experiments, for instance). In a previous publication [17], we determined in which conditions the longitudinal order and the polarization difference were created and the goal of the present work is naturally to devise a procedure for creating a net hyperpolarization. Before describing this procedure (a particular pulse sequence), we shall study the relaxation properties of the polarization difference in order to determine a possible delay between the insertion of the sample in the NMR magnet and the start of the NMR experiment. Finally, the evolution of the net polarization (and of the existing longitudinal order with possible coupling between them), which is of prime

* Corresponding author. Fax: +33 3 83 68 43 47.
E-mail address: Daniel.Canet@crm2.uhp-nancy.fr (D. Canet).

1090-7807/$ - see front matter © 2011 Elsevier Inc. All rights reserved.
doi:10.1016/j.jmr.2011.02.017

importance in view of many applications (notably as far as imaging experiments are concerned), will be considered experimentally and justified theoretically.

The model we are going to use in this study originates from methyl-d^3 butynoic acid in acetone-d^6 as shown in Fig. 1 [17].

The advantage of this molecule is that it is almost a perfect two-spin system if we neglect possible transfers toward the deuterated methyl directly bound to the double bond. We were able to show both theoretically and experimentally that, with a classical ALTADENA experiment (reaction carried out in the earth field), besides the longitudinal order $2I_z^AI_z^B$, even a larger amount of polarization was created but in the form of a *polarization difference* $(I_z^A - I_z^B)$. This is evidenced by the spectra of Fig. 2, owing to the fact that both $2I_z^AI_z^B$ and $(I_z^A - I_z^B)$ are observable by means of a $\pi/4$ pulse while a $\pi/2$ unravels only $(I_z^A - I_z^B)$.

Thus, upon insertion of the sample in the magnet, an enhanced polarization difference (several orders of magnitude larger than the thermal polarization) is available.

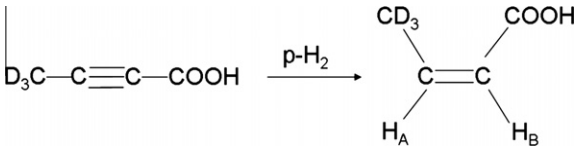

Fig. 1. The model molecule used in this work. It was obtained using an acetone-d^6 solution (0.4 ml) of $[Rh(NBD)dppb]^+[BF_4]^-$ (20 mM) as catalyst and methyl-d^3 butynoic acid (480 mM). Para-H_2 was enriched cooling H_2 in liquid nitrogen (77 K) with activated charcoal as ortho-para conversion catalyst. The para-hydrogenation reactions were carried out by shaking the NMR tube (gas tight NMR tubes equipped with Young valve) previously charged with 4 atm of parahydrogen out of the NMR spectrometer (ALTADENA experiment). All the spectra were acquired on a Bruker Avance 600 MHz spectrometer.

2. Relaxation of polarization difference by intramolecular proton relaxation

This is the relaxation behavior between the two hyperpolarized *A* and *B* protons. The relevant Solomon equations can be written as

$$\begin{aligned}\frac{dI_z^A}{dt} &= -R_1^A(I_z^A - I^{eq}) - \sigma_{AB}(I_z^B - I^{eq})\\ \frac{dI_z^B}{dt} &= -R_1^B(I_z^B - I^{eq}) - \sigma_{AB}(I_z^A - I^{eq})\end{aligned} \quad (1)$$

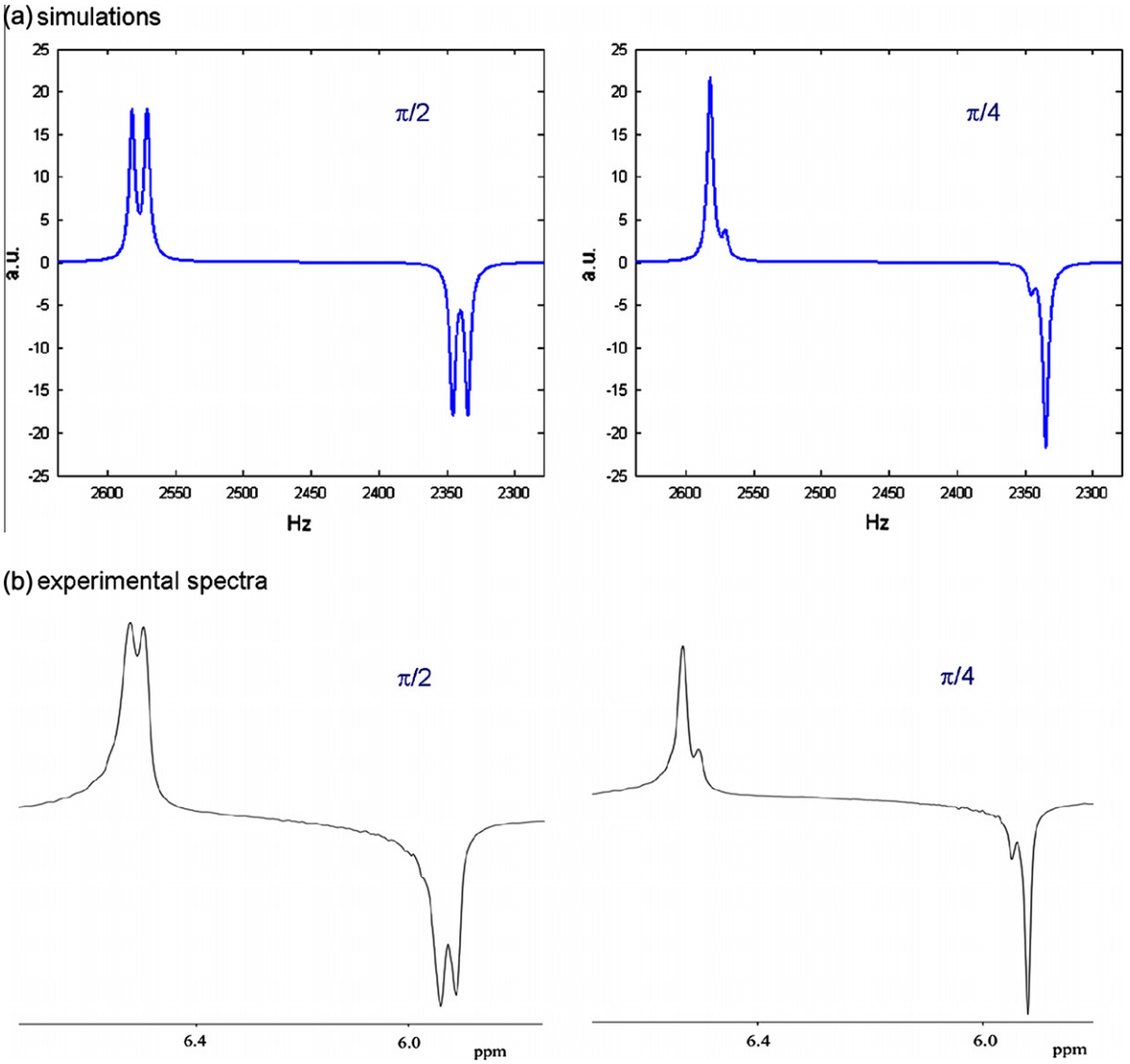

Fig. 2. Spectra showing the formation of enhanced spin states (ALTADENA experiment): $2I_z^AI_z^B$ and $(I_z^A - I_z^B)$. Left: only $(I_z^A - I_z^B)$. Right: both $2I_z^AI_z^B$ and $(I_z^A - I_z^B)$. From Ref. [17].

With R_1^A and R_1^B the longitudinal relaxation rate of A and B respectively, and σ_{AB} the cross-relaxation rate between A and B.

Defining D and S as

$$D = I_z^A - I_z^B \\ S = I_z^A + I_z^B \quad (2)$$

and recognizing that we are primarily interested in the evolution of D, we obtain

$$\frac{dD}{dt} = \left(\frac{-R_1^A + R_1^B}{2}\right)S - \left(\frac{R_1^A + R_1^B}{2}\right)D + (R_1^A - R_1^B)I^{eq} + \sigma_{AB}D \quad (3)$$

Owing to the fact that $R_1^A \approx R_1^B$ (this relaxation rate will be denoted R_1), that S remains small and that I^{eq} is always much smaller than D, we arrive at

$$\frac{dD}{dt} = -(R_1 - \sigma_{AB})D \quad (4)$$

If we further assume that extreme narrowing conditions prevail and that the dipolar interaction between A and B is the dominant relaxation mechanism, $\sigma_{AB} \approx R_1/2$ and

$$\frac{dD}{dt} = -\frac{R_1}{2}D \quad (5)$$

Therefore the polarization difference evolves according to a relaxation time which is twice the relaxation time of A or B. This can be easily checked by monitoring the proton system with a $\pi/2$ pulse occurring at different intervals subsequently to the insertion of the sample into the NMR magnet. As these experiments are one-shot in nature, this requires unfortunately to repeat the hydrogenation reaction for each mixing time and we can just hope to obtain an approximate value of the effective relaxation time of D.

This has been checked by normal inversion recovery experiments performed on the molecule in the right part of Fig. 1 lead to a T_1 value of 19 s for the ethylenic protons while the evolution of D measured as indicated above lead to a effective T_1 value of 40 s. These results confirm the trend predicted by the above calculations.

3. Transforming enhanced polarization difference into net hyperpolarization

The conversion of $(I_z^A - I_z^B)$ into $(I_z^A + I_z^B)$ can be accomplished by the following sequence which is applied subsequently to the insertion of the sample into the NMR magnet.

$$(\pi/2)_x - 1/2\Delta\nu - (\pi/2)_y \quad (6)$$

For this sequence, the carrier frequency has to be set at $(\nu_A + \nu_B)/2$, where ν_A and ν_B are the resonance frequencies of spins A and B, respectively and with $\Delta\nu = \nu_A - \nu_B$. Note that this sequence only works for a two-spin system (as illustrated by the scheme of Fig. 3), hence the interest of our parahydrogenated molecule.

This has been checked by the experimental results shown in Fig. 4.Also, it is easy to see that this pulse sequence transforms the longitudinal order $2I_z^AI_z^B$ into its opposite. Thus, as considered in the following section, the longitudinal order invariably created by the hydrogenation reaction is not destroyed and is therefore prone to evolve and even couple with polarizations.

4. Evolution of net hyperpolarization

Before considering potential applications of this net hyperpolarization, it is important to determine its duration, that is to monitor its relaxation. This evolution has been followed by the following sequence

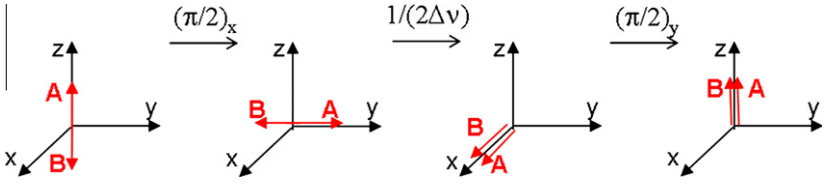

Fig. 3. Effect of the pulse sequence (6).

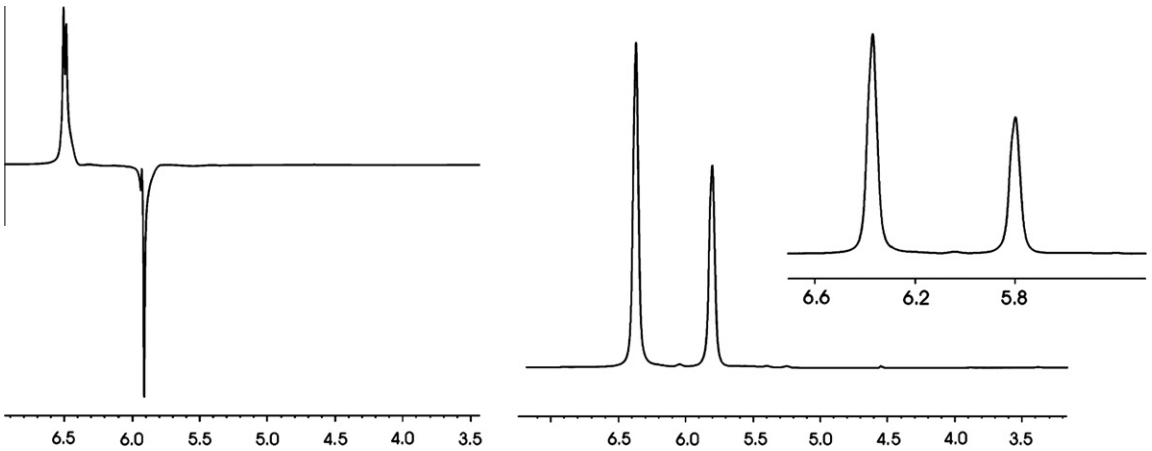

Fig. 4. Left: spectrum resulting from the application of a $\pi/2$ pulse after the ALTADENA experiment showing that the latter produces effectively a polarization difference. Right: the same spectrum after application of sequence (6) followed by an interval of 3 s before the final $\pi/2$ read-pulse. A net polarization is created but with a noticeable intensity difference between the two spins, attributable to transverse relaxation phenomena or to long-range J coupling effects, or to an imperfect setting of the carrier frequency.

$$(\pi/2)_x - 1/2\Delta\nu - (\pi/2)_y - \tau_1 - (\alpha) - Acq_1 - \tau_2 - (\alpha) - Acq_2 - \tau_3 - (\alpha) - Acq_3 \quad (7)$$

where α represents a small flip angle pulse (2° for the experiments shown below). We shall make the approximation that this small angle read-pulse does not significantly affect the evolution of the different spin states appearing subsequently to sequence (6). Now, let x be the phase of the α pulse. It can be seen that I_z^A is transformed in the observable quantity αI_y^A while the observable quantities arising from $2I_z^A I_z^B$ are $\alpha(2I_y^A I_z^B + 2I_z^A I_y^B)$, thus two anti-phase doublets. Experimental results are shown in Fig. 5. It can be realized that (i) owing to the visible contribution of anti-phase doublets, the longitudinal order is involved in this evolution, (ii) part of the hyperpolarization is long-lived.

For interpreting these experimental observations, we shall first consider the integral of each doublet. In that way, the effect of longitudinal order is *ipso facto* suppressed since the integral of the corresponding anti-phase doublet is zero. Now, let us define A by $A = I_z^A - I_{eq}^A$ and B by $B = I_z^B - I_{eq}^B$ and $A(0) = K_A$, $B(0) = K_B$, K_A and K_B being possibly much greater than the equilibrium values (if they have been hyperpolarized, as this is the case here). Thus, Solomon equations (see (1) for the meaning of the different symbols) can be written as

$$\begin{aligned} \frac{dA}{dt} &= -R_1^A A - \sigma_{AB} B \\ \frac{dB}{dt} &= -R_1^B B - \sigma_{AB} A \end{aligned} \quad (8)$$

Their solution is as follows

$$\begin{aligned} A &= a_+ e^{\lambda_+ t} + a_- e^{\lambda_- t} \\ B &= b_+ e^{\lambda_+ t} + b_- e^{\lambda_- t} \end{aligned} \quad (9)$$

λ_+ and λ_- are both negative and are expressed as

$$\lambda_\pm = -\frac{R_1^A + R_1^B}{2} \pm \frac{1}{2}\sqrt{(R_1^A - R_1^B)^2 + 4\sigma_{AB}^2} \quad (10)$$

The coefficients depend on all relaxation parameters and, of course, on the initial conditions. One has

$$\begin{aligned} b_+ &= -\frac{\sigma_{AB}}{\lambda_+ + R_1^B} a_+ \\ b_- &= -\frac{\sigma_{AB}}{\lambda_- + R_1^B} a_- \end{aligned} \quad (11)$$

and

$$\begin{aligned} a_+ &= \frac{K_A/(\lambda_- + R_1^B) + K_B/\sigma_{AB}}{1/(\lambda_- + R_1^B) - 1/(\lambda_+ + R_1^B)} \\ a_- &= \frac{K_A/(\lambda_+ + R_1^B) + K_B/\sigma_{AB}}{1/(\lambda_+ + R_1^B) - 1/(\lambda_- + R_1^B)} \end{aligned} \quad (12)$$

The crucial point arises from λ_+ which may become very small, thus leading to *long lived proton hyperpolarized molecules*.

In order to understand qualitatively this latter feature, we shall use the approximations already put forward (i.e. $R_1^A = R_1^B = R_1$, $\sigma_{AB} = R_1/2$), we obtain

$$\begin{aligned} &\lambda_+ = -R_1/2 \quad \lambda_- = -3R_1/2 \\ &a_+ = (K_A - K_B)/2 \quad b_+ = -a_+ \\ &a_- = (K_A + K_B)/2 \quad b_- = a_- \end{aligned} \quad (13)$$

The value of λ_- is akin to the 3/2 effect [18]. It can be seen that the contribution of the longest relaxation time ($1/\lambda_+$) depends on the difference in initial values of A and B hyperpolarization. On the other hand, $b_+ = -a_+$, meaning that the long-lasting hyperpolarization for A and B would be of opposite sign, thus a hyperpolarization difference as the one observed immediately after the hydrogenation reaction (see Fig. 4, left) and we retrieve the relaxation rate pertaining to D (see equation (5)). These conclusions can however be modified if R_1^A and R_1^B are no longer identical and if σ_{AB} is smaller than in the above calculations.

The next stage is to deal with exact values of R_1^A, R_1^B, σ_{AB} and to a possible coupling between longitudinal order and polarizations (by means of csa-dipolar cross-correlation terms). Eq. (8) have to be amended as follows:

$$\begin{aligned} \frac{dA}{dt} &= -R_1^A A - \sigma_{AB} B - \sigma_{csa(A),d} C \\ \frac{dB}{dt} &= -R_1^B B - \sigma_{AB} A - \sigma_{csa(B),d} C \\ \frac{dC}{dt} &= -R_1^C C - \sigma_{csa(A),d} A - \sigma_{csa(B),d} B \end{aligned} \quad (14)$$

$\sigma_{csa(A),d}$ and $\sigma_{csa(B),d}$ are the so-called cross-correlation terms (depending on the csa mechanism and on the dipolar interaction

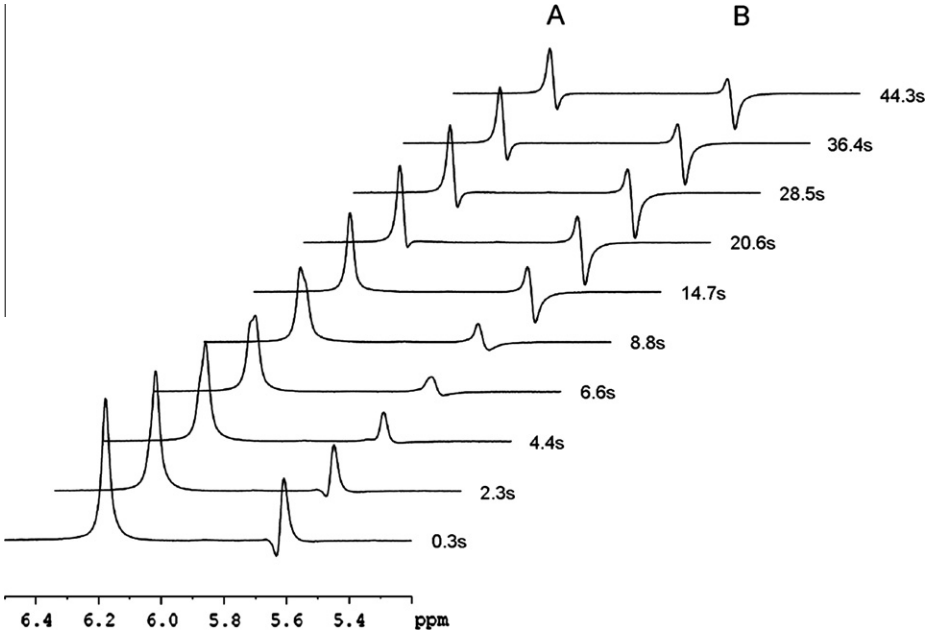

Fig. 5. Evolution of a spectrum similar to the one of Fig. 4 (right) probed by sequence (7). The contribution of anti-phase doublets arising from the spin longitudinal order is clearly visible in some spectra while, in others, only one line of the doublet appears.

between A and B) which couple the longitudinal spin order and A or B polarization [19,20]. R_1^C is the specific longitudinal spin order relaxation rate. A is defined by $A = I_z^A - I_{eq}^A$ and B by $B = I_z^B - I_{eq}^B$ as previously, and $C = 2I_z^A I_z^B$ is the longitudinal order.

Experiments (see Fig. 5) have shown that Eq. (14) had to be amended so as to take into account the creation of C according to a "PASADENA effect". Indeed, it turned out that the hydrogenation reaction continued once the sample in the NMR magnet, so PASADENA effect (creation of longitudinal order) had to be added to the ALTADENA one. Last Eq. of (14) becomes:

$$\frac{dC}{dt} = -\sigma_{csa(A),d}A - \sigma_{csa(B),d}B - k(1-K)C(0)\exp(-kt) - KR_1^C C(0)\exp(-R_1^C t) \quad (15)$$

With k the edification rate of C by PASADENA, and $KC(0)$ the quantity created at the achievement of the hydrogenation reaction after the insertion of the sample into the NMR magnet.

5. Interpretation of experimental data

The series of spectra of Fig. 5 has been analyzed first by considering the integral of the two A and B patterns, thus avoiding the contribution of anti-phase doublets (as explained above). This analysis provides a first approximation for $R_1^A, R_1^B and \sigma_{AB}$. In a second step, each pattern was deciphered according to in-phase and anti-phase doublets. As the anti-phase doublets reflect the longitudinal order, it becomes possible to access its evolution and therefore to treat the whole data set according to (14) by trial-and-error. Although the accuracy of the parameters derived that way is not warranted, the relaxation rates (see Fig. 6 caption) are of the expected order of magnitude. Theoretical curves together with the experimental data points are shown in Fig. 6. The agreement is quite satisfactory and confirms the validity of Eq. (14). This has been further confirmed by an independent experiment (not shown) carried out with an open sample tube so as to minimize the continuation of the hydrogenation reaction (PASADENA effect). This experiment yields similar relaxation parameters. Another point worth mentioning is the initial negative value of the longitudinal order (as predicted by analyzing the effect of sequence (6)) and its rapid growing due to the continuation of the hydrogenation reaction. As a matter of fact, PHIP is well known for its ability to unravel reaction kinetics or complex reaction pathways [1], especially through long-lasting hyperpolarization [15,21,22] and possibly by accounting for magnetic field effects [23,24].

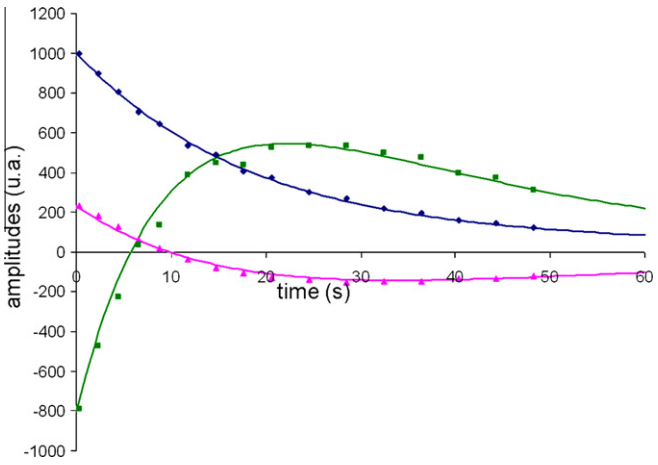

Fig. 6. Decay of A (diamonds) and B (triangles) polarizations (see Fig. 5) and build-up of the longitudinal order C (squares). The horizontal axis represents the time elapsed from the end of subsequence (6). Relaxation rates in s^{-1} are as follows: $R_1^A = R_1^B = 0.048, \sigma_{AB} = 0.024, R_1^{AB} = 0.030, \sigma_{csa(A),d} = 0.004, \sigma_{csa(B),d} = 0.004$..

6. Conclusion

The first aim of the present work was to obtain a net hyperpolarization subsequently to a para-hydrogenation reaction with the prospective to transfer this hyperpolarization to other molecules present in the solution. To a certain extent, this objective could be related to the recently proposed SABRE method [25]. This implies however to understand the time evolution of this global hyperpolarization. In spite of an apparent complexity (see Fig. 5), it turns out that extended Solomon equations, including polarizations and longitudinal spin order, allowed us to perfectly interpret experimental data.

References

[1] J. Natterer, J. Bargon, Parahydrogen induced polarization, Prog. Nucl. Magn. Reson. Spectrosc. 31 (1997) 293–315.
[2] K. Golman, O. Axelsson, H. Johannesson, S. Mansson, C. Olofsson, J.S. Petersson, Parahydrogen-induced polarization in imaging: subsecond ^{13}C angiography, Magn. Reson. Med. 46 (2001) 1–5.
[3] S.B. Duckett, C.L. Newell, R. Eisenberg, More than INEPT: parahydrogen and INEPT+ give unprecedented resonance enhancement to ^{13}C by direct ^{1}H polarization transfer, J. Am. Chem. Soc. 115 (1993) 1156–1157.
[4] J. Barkemeyer, J. Bargon, H. Segstschmid, R. Freeman, Heteronuclear polarization transfer using selective pulses during hydrogenation with parahydrogen, J. Magn. Reson. A 120 (1996) 129–132.
[5] M. Haake, J. Natterer, J. Bargon, Efficient NMR pulse sequences to transfer the para-hydrogen-induced polarization to heteronuclei, J. Am. Chem. Soc. 118 (1996) 8688–8691.
[6] M. Roth, A. Koch, P. Kindervater, J. Bargon, H.W. Spiess, K. Münnemann, ^{13}C hyperpolarization of a barbituric acid derivative via parahydrogen induced polarization, J. Magn. Reson. 204 (2010) 50–55.
[7] F. Reineri, A. Viale, G. Giovenzana, D. Santelia, W. Dastrù, R. Gobetto, S. Aime, New hyperpolarized contrast agents for ^{13}C-MRI from para-hydrogenation of oligooxyethylenic alkynes, J. Am. Chem. Soc. 130 (2008) 15047–15053.
[8] M. Goldman, H. Jóhannesson, Conversion of a proton pair para order into ^{13}C polarization by rf irradiation, for use in MRI, C. R. Phys. 6 (2005) 75–581.
[9] M. Goldman, H. Jóhannesson, O. Axelsson, M. Karlsson, Design and implementation of ^{13}C hyperpolarization from para-hydrogen, for new MRI contrast agents, C. R. Chimie 9 (2006) 357–363.
[10] P. Bhattacharya, E.D. Chekmenev, W.H. Perman, K.C. Harris, A.P. Lin, V.A. Norton, C.T. Tan, B.D. Ross, D.P. Weitekamp, Towards hyperpolarized ^{13}C-succinate imaging of brain cancer, J. Magn. Reson. 186 (2007) 150–155.
[11] E.D. Chekmenev, J. Hövener, V.A. Norton, K.C. Harris, L.S. Batchelder, P. Bhattaccharya, B.D. Ross, D.P. Weitekamp, J. Am. Chem. Soc. 130 (2008) 4212–4213.
[12] E.D. Chekmenev, V.A. Norton, D.P. Weitekamp, P. Bhattaccharya, Hyperpolarized ^{1}H NMR employing low γ nucleus for spin polarization storage, J. Am. Chem. Soc. 131 (2009) 3164–3165.
[13] (a) C.R. Bowers, D.P. Weitekamp, Transformation of symmetryzation order to nuclear spin magnetization by chemical reaction and nuclear magnetic resonance, Phys. Rev. Lett. 57 (1986) 2645–2648;
(b) C.R. Bowers, D.P. Weitekamp, Parahydrogen and synthesis allow dramatically enhanced nuclear alignment, J. Am. Chem. Soc. 109 (1987) 5541–5542.
[14] M.G. Pravica, D.P. Weitekamp, Net NMR alignment by adiabatic transport of para-hydrogen addition products to high magnetic field, Chem. Phys. Lett 145 (1988) 255–258.
[15] T. Jonischkeit, U. Bommerich, J. Stadler, K. Woelk, H.G. Niessen, J. Bargon, Generating long-lasting ^{1}H and ^{13}C hyperpolarization in small molecules with parahydrogen-induced polarization, J. Chem. Phys. 124 (2006) 201109.
[16] D. Canet, S. Bouguet-Bonnet, C. Aroulanda, F. Reineri, About long-lived nuclear spin states involved in par-hydrogenated molecules, J. Am. Chem. Soc. 129 (2007) 1445–1449.
[17] S. Bouguet-Bonnet, F. Reineri, D. Canet, Effect of the static magnetic field strength on parahydrogen induced polarization NMR spectra, J. Chem. Phys. 130 (2009) 234507.
[18] A. Abragam, The Principles of Nuclear Magnetism, Oxford University Press, London, 1961.
[19] D. Canet, Nuclear Magnetic Resonance: Concepts and Methods, Wiley, Chichester, 1996.
[20] J. Kowalewski, L. Mäler, Nuclear spin relaxation in liquids: theory, experiments, and applications, Taylor & Francis, 2006.
[21] J. Natterer, O. Schedletzky, J. Barkemeyer, J. Bargon, S.J. Glaser, Investigating catalytic processes with para-hydrogen: evolution of zero-quantum coherence in AA'X spin systems, J. Magn. Reson. 133 (1998) 92–97.

[22] P. Hubler, R. Giernoth, G. Kummerle, J. Bargon, Investigating the kinetics of homogeneous hydrogenation reactions using PHIP NMR spectroscopy, J. Am. Chem. Soc. 121 (1999) 5311–5318.
[23] K.L. Ivanov, A.V. Yurkovskaya, H.-M. Vieth, Coherent transfer of hyperpolarization in coupled spin systems at variable magnetic fields, J. Chem. Phys. 128 (2008) 154701.
[24] S.E. Korchak, K.L. Ivanov, A.V. Yurkovskaya, H.-M. Vieth, Para-hydrogen induced polarization in multi-spin systems studied at variable magnetic field, Phys. Chem. Chem. Phys. 11 (2009) 11146–11156.
[25] R.W. Adams, J.A. Aguilar, K.D. Atkinson, M.J. Cowley, P.I.P. Elliott, S.B. Duckett, G.G.R. Green, I.G. Khazal, J. Lopez-Serrano, D.C. Williamson, Science 323 (2009) 1708–1711.